Symmetric-charge-transfer cross sections for gadolinium in the energy range 10–1000 eV

Shuji Sakabe, Yasukazu Izawa, Masaki Hashida, and Sadao Nakai
Institute of Laser Engineering, Osaka University, Suita Osaka 565, Japan

Chiyoe Yamanaka
Institute for Laser Technology, Suita Osaka 565, Japan
(Received 2 January 1991; revised manuscript received 7 May 1991)

The cross section of symmetric charge transfer between Gd and Gd^+ as a function of impact energy (velocity) in the range of 10–1000 eV (3.5×10^5–3.5×10^6 cm/sec) was successfully obtained by a crossed-beam technique, which featured a pulsed ion beam produced by laser photoionization in an atomic gas beam. The absolute values and the impact-energy dependence of the cross sections were obtained from the attenuation rate of the primary ions in the atomic gas and the ratio of the detected charge transferred ions to the primary ions, respectively. The cross sections obtained are larger than those of other elements studied in the past, and the impact-velocity–cross-section curve could be fitted with that obtained from the superposition of the resonant and capture-type probabilities resulting in charge transfer, assuming that the capture-type cross section is inversely proportional to the impact velocity.

PACS number(s): 34.70.+e, 82.30.Fi

I. INTRODUCTION

Symmetric charge transfer between an atom and a positive atomic ion has been investigated in detail both experimentally and theoretically since the 1930s [1]. The features of the cross-section–impact-velocity curves obtained experimentally can be interpreted by theoretical calculations. These symmetric charge-transfer cross sections are well explained by resonant processes. However, in spite of the seeming abundance of investigations on symmetric charge transfer, the experimental data, especially for elements with complicated electron configurations, such as transition elements, are still scanty, and none are available for elements except for hydrogen, alkali-metal, alkaline-earth, and rare-gas elements. The present work has been motivated by the lack of data and additionally by the significance of this collision in atomic vapor laser isotope separation (AVLIS) for metallic elements [2]. In AVLIS, the charge-transfer collisions between selectively laser-photoionized target elements and major elements in a metal gas reduce the selectivity that is the enrichment factor of the target elements, because charge-transferred major elemental ions are also collected. Therefore, the cross sections of charge transfer for metallic elements are crucial to estimating feasibility for AVLIS. The present paper gives the cross section of the symmetric charge transfer in the range 10–1000 eV for gadolinium, which is useful as a burnable poison in a fission reactor. This was obtained by a crossed-beam technique which featured a pulsed dense ion beam produced by laser photoionization.

II. EXPERIMENTAL METHOD

In standard experiments that measure the charge-transfer cross section for a metallic element, a crossed-beam apparatus is used, in which the cross section is determined from the ratio between the numbers of charge-transferred ions and the injected primary ions. In such a device, charge-transferred ions stream in the same direction as the primary atoms after the interaction. The charge-transferred ions must be separated from the primary atomic beam after they leave, requiring that the ion detector's gain, coupled with the collection efficiency, is absolutely calibrated. On the other hand, for a gas element, an attenuation method is standard, by which the cross section is determined from the attenuation rate of the injected primary-ion beam through the atomic gas. Although, in this case, the product of the collision length and the atomic gas density is sufficient for measurement of the attenuation rate of the injected-ion beam, the current ratio between the injected- and attenuated-ion beams allows determination of the cross section and, therefore, absolute sensitivity is not required from the detector. We have used both the former and latter techniques to determine the degree of dependence of the cross sections on the impact energy in the range of 100–1000 eV, and to measure the absolute cross section in the energy range 10–200 eV, respectively. We also found that these two measurements are interconnected.

The crossed-beam technique used in the present work is reported in detail in Ref. [3]. Here we present only a brief explanation for the experiment

$$Gd^+ + Gd \rightarrow Gd + Gd^+ .$$

A high-density beam of metallic atoms was produced by vaporization in a crucible located in the first of two differentially pumped vacuum chambers. Fifty grams (50 g) of Gd metal in a 10-cm^3 Ta crucible was heated with an electron-beam gun (1830–1900 K at a power density of 340–450 W/cm^2). A schematic view of the crossed-beam apparatus to measure charge-transferred ions is shown in Fig. 1(a). The apparatus was located in the

second chamber. The neutral beam emerged from an orifice in the wall separating the first and second chambers and passed through a collimating aperture in the wall of a box isolating the beam interaction region. As the beam (labeled B1 in Fig. 1) proceeded into the interaction box, it first passed between a pair of paralleled deflecting magnets used to remove charged particles coming from the crucible and accompanying the atoms in the beam, after which the atomic beam was crossed by a pulsed ion beam in an interaction region. The ion-beam source was produced by photoionization in the other atomic beam (B2 in Fig. 1). The atomic beam for the ion source was generated in the same crucible as that for the atomic beam B1 and emerged through another aperture from another orifice located adjacent to the above-mentioned aperture and orifice, respectively, after which the atomic beam was partially photoionized by focused ArF pulsed laser light. The laser energy was 100 mJ, the pulse duration 21 nsec, and the repetition rate 30 Hz. Ions produced were extracted from the atomic beam B2 by a static electric field applied between a pair of electrodes, located on either sides of the laser-beam–atomic-beam interaction region, and focused as a pulsed-ion beam on the atomic beam B1 by means of an ion lens. The ion-beam–atomic-beam interaction region was shielded by a pair of plates located on each of its both sides. The ion lens was simply constructed by an aperture in one of the electrodes and a meshed aperture in the plate. Before a collision experiment, the species of the ion beam was identified by a Q-mass filter located through a hole on the far plate. The number of ions to collide with the atomic beam B1 was monitored by means of a collector plate, which could be positioned in place of the far shielding plate, connected to a data-acquisition system. Ions produced by charge-transfer collisions stream upwards as fast as the atoms in the beam B1. They were focused by an ion lens located above the interaction region and guided toward an ion detector [a ceramic electron multiplier (CEM)] by a static electric field applied by curved grating electrodes. To identify the detected ions, a shutter was located between the orifice and the aperture in each atomic beam (S1 and S2 in Fig. 1). The signal of charge-transferred ions was not observed when S1 and/or S2 were closed. Pulsed noise included in the primary ion signal due to residual gas and cw noise in the charge-transferred ion signal due to charged particles (mainly electrons) in atomic beam B1 were measured by closing S2 and S1, respectively. The atomic-beam density was monitored by a vapor monitor located above the region of laser-beam-atomic-beam interaction.

The schematic view of the apparatus to measure the attenuation of the primary ions is shown in Fig. 1(b). The configuration is essentially the same as that shown in Fig. 1(a), except that atomic beam B1 is so large that the attenuation of the injected primary ions in the atomic gas is measurable. The atomic beam could be switched by a shutter located between the orifice and the aperture, and the injected ion beam was measured with the shutter closed. The ion beam passed through the atomic gas and impinged on an ion collector. The detection surface of

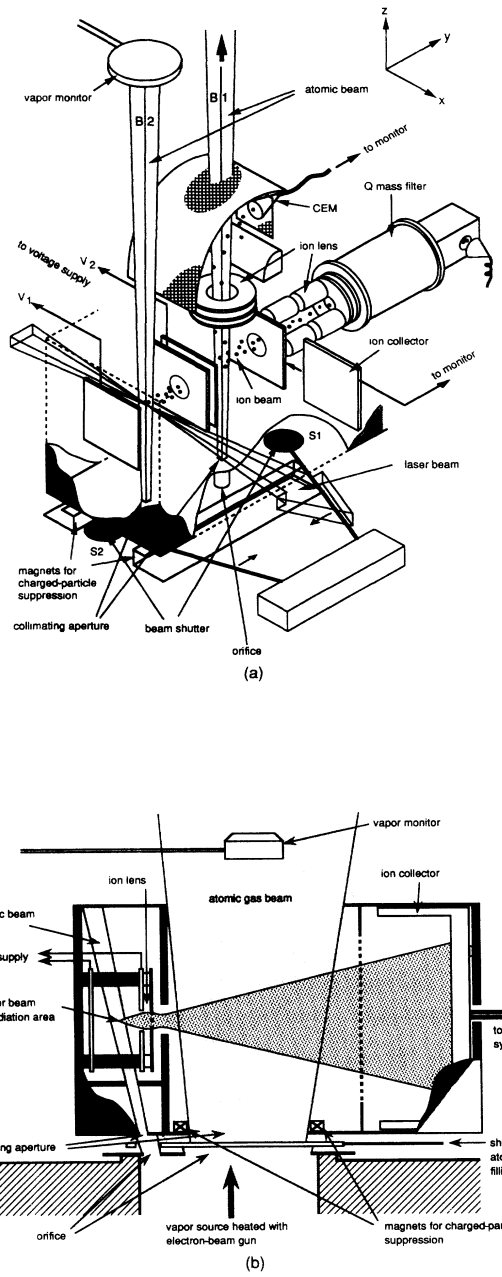

FIG. 1. Schematic views of the apparatus for measuring of charge-transfer cross sections using a crossed-beam technique. The two atomic beams emerged from orifices on the floor separating the first and second chambers. The crucible and electron-beam gun for atomic vapor production are located in the first chamber (not seen in this figure), which is situated below the second chamber. A laser beam is injected into one of the atomic beams, which photoionizes it, and the ions produced are extracted and focused onto another atomic beam. Both (a) the charge-transferred ions and (b) the attenuation of the primary ions are measured. In (a) the charge-transferred ions are guided by curved electrodes through an ion lens, and are detected by a ceramic-type electron multiplier. In (b), the injected primary ions and the attenuated ions are alternately detected by a Faraday cup, closing and opening a shutter for the atomic-beam gas, respectively.

the ion collector was designed to be large enough for all of the ion beam, which was subject to spreading by the space-charge effect, to be detected. The noise level of the ion-collector signal was created by mainly secondary electrons emitted from the electron-beam-heated vapor source in the crucible, because of the use of the large orifice and collimating aperture. The noise level fluctuates with the same frequency as the thyrister that controls the current of the electron-beam gun. In order to reduce the effect of the noise, the primary-pulsed-ion-beam injection, that is, the laser-light irradiation, was triggered at the same frequency (60 Hz). The atomic-beam density was monitored by a vapor monitor in the atomic gas beam.

The atomic-beam density n was determined by the beam flux f and the atomic-beam velocity v, with $n=f/v$. Atomic-beam flux was measured with a vapor monitor (quartz oscillator type), which is a calibrated commercial device. The thermal velocity of the atomic beam was obtained by the temperature of the atomic vapor source, measured by an ir radiation thermometer. By measuring the beam sizes at the interaction region and the position of the vapor monitor, the density at the interaction region was successfully obtained from that at the vapor monitor. The interaction length, that is, the target length, was obtained by a separate measurement of the density profile for the atomic beam that coated a glass plate that was located at the interaction region.

All ion-current signals from the apparatus mentioned above were digitized after adequate amplification and transferred into a microcomputer. Quick data acquisition is crucial in these crossed-beam apparatus, because the reduction of material in the crucible sensitively affects both the atomic-beam density and collision length. A repetitive pulsed laser combined with a fast-response digitizer makes it possible to reduce the acquisition time required to obtain one dependent set of data to a duration shorter than the characteristic beam-source reduction time.

III. APPARATUS TEST

As mentioned above, the signal from the CEM is surely for ions generated by the collisional process at the interaction region of crossed beams, because no signal was observed when atomic beams B1 and/or B2 were turned off by closing shutters S1 and/or S2, respectively, or the laser irradiation was turned off.

Besides charge-transfer collisions, there are possible collisions which allow some ions to flow into the CEM as in the case of the method used to measure charge-transferred ions, or which affect the number of primary ions that reach the collector through the atomic gas as in the case of the attenuation method; these include (a) elastic collision, (b) Coulomb collision (ion-ion, ion-electron), (c) electron-impact ionization, and (d) recombination (three-body photon and electron). Possibilities (c) and (d) can be ignored because of small cross section ($<10^{-16}$ cm^2) and low electron density in the atomic beam. For possibility (a) the cross section can be estimated to be approximately 1.8×10^{-15} cm^2, assuming that the effective radius of the Gd atom is equal to that of uranium, 2.4 Å [4]. The cross section of collision (b), by which the injected primary ions are scattered out of the ion collector for the attenuation method, is calculated to be approximately $3.8\times10^{-12}\varepsilon^{-2}$ for $Gd^+ + Gd^+$ and $9.4\times10^{-13}\varepsilon^{-2}$ for $Gd^+ + e$, where ε is the impact energy in eV. These cross sections are less than the cross sections obtained (mentioned later) in the range 10–1000 eV. Additionally, the ion density in the atomic beam is much less than the atomic density. Therefore, it can be concluded that the cross sections obtained are for charge-transfer collision.

In order to test the function of the present apparatus and to gain the confidence for its use, we have measured an element whose cross section has never been studied in another work in the past. The metallic elements studied most intensively are alkali metals, and alkaline-earth elements also have been measured, though much less intensively than alkali-metal elements. The present technique, by which the atomic beam is produced by electron-beam heating and the ion beam is generated by ArF-laser photoionization, cannot be applied to alkali-metal elements without any modification (such as Joule heating with tungsten-resistance and well-tuned dye lasers) because melting points of alkali-metal elements are much lower than that of Gd, and well-controlled vaporization is difficult, and, additionally, the alkali-metal elements that have no autoionization levels cannot be ionized by a single photon of the ArF laser. For this reason, we have chosen the alkaline-earth element Ca as the test element. It is even difficult to control the vaporization of Ca. Therefore, the number of energies at which the cross sections can be measured is limited, while the dependence for Gd was almost continuously measured, because the number of laser shots must be sufficient for the effect of atomic density fluctuation to be averaged. Absolute measurement by the attenuation method was also done at only one fixed energy, 100 eV.

Seven grams (7g) of Ca metal in a 10-cm^3 Ta crucible was used, and the power density of the electron beam was 40 W/cm^2. As will be mentioned later, the cross sections of Ca obtained show fairly good agreement with the result of the experiment done by Panev *et al.* [5] and theoretical prediction [1]. Technical confidence in the present apparatus was obtained.

IV. RESULTS

The charge-transfer cross section $\sigma(\varepsilon)$ at impact energy ε is obtained from

$$\sigma(\varepsilon)=-\frac{1}{nl}\ln\left[\frac{N}{N_{CT}+N}\right]=-\frac{1}{nl}\ln\left[\frac{N}{N_0}\right],$$

where N_{CT}, N, and N_0 are the numbers of the charge-transferred ions, the attenuated ions, and the injected primary ions, respectively, n is the number density of the atomic gas beam, and l is the collision length along the ion-beam path. In the apparatus shown in Fig. 1(a), αN_{CT} and N ($\approx N_0$) were measured simultaneously with 100 (Gd) and 500 (Ca) laser shots at each impact energy, where α is the detector's gain coupled with the collection efficiency. n was 10^{10} cm^{-3} (Gd) and 10^{11} cm^{-3} (Ca) and

l was 3.2 mm. In the apparatus in Fig. 1(b), N_0 and N were measured alternatively with 2000 (Gd) and 10 000 (Ca) shots for each energy, under the conditions of $n=10^{11}$ cm^{-3} and $l=85$ mm. In both cases, the ion-beam energy ε was changed by the potentials applied on the electrodes for ion-beam extraction from the ion source.

Before measuring the cross sections, the dependence of the quantity of charge-transferred ions on collisional length (nl) was measured in order to verify that the ion signal is really due to the collision events in the crossed-beam region. Here the atomic-beam density n was changed. Figure 2 shows N_{CT}/N_0 versus n for the Gd experiment with the crossed-beam apparatus. The proportionality of N_{CT}/N_0 to n was clearly seen, thereby supporting the relation $N_{CT}\approx N_0 n\sigma l$.

In Fig. 3 the measured cross sections are shown. For Gd the scatter of data obtained by the attenuation method [open circles in Fig. 3(a)] is due to the small attenuation of the primary-ion beam (3–5%). However, the absolute values of the cross sections were successfully measured without any assumption on other atomic data. As shown in Ref. [3], α ($=11\%$) can be calibrated, and the cross sections obtained with the measured α were successfully correlated with those obtained using the attenuation method. Here, however, the energy dependence obtained by charge-transferred-ion measurement was coupled with the absolute values of the cross sections obtained using the attenuation method, in the energy interval 100–200 eV, because the cross sections obtained using the attenuation method are more reliable than those by the charge-transferred-ion measurement.

It should be noted that the atoms and ions in the present beams do not lie in the ground state, but rather in some excited state close to the ground state. The characteristics of the atomic and ion beams are determined by the production process, that is, atomic vapor production by electron-beam heating and subsequent ion production by laser photoionization. The primary atoms are emitted from the high-temperature liquid in the crucible, and may be collisionally excited. The temperature of the Gd atomic-beam source (1900 K) measured by an ir radiation thermometer allows us to calculate that the atoms are populated by collisional processes into the states of

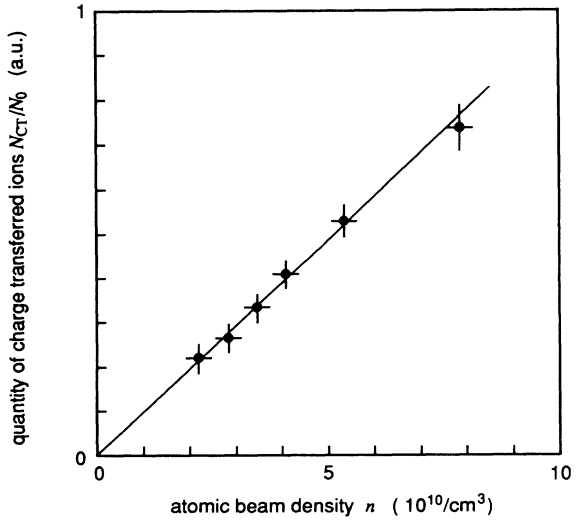

FIG. 2. Dependence of the quantity of charge-transferred ions, N_{CT}/N_0, on the collisional length (nl) at an impact energy of 300 eV for the Gd experiment with the crossed-beam apparatus. The proportionality of N_{CT}/N_0 to n was so clearly seen that it supports the relation $N_{CT}\approx N_0 n\sigma l$.

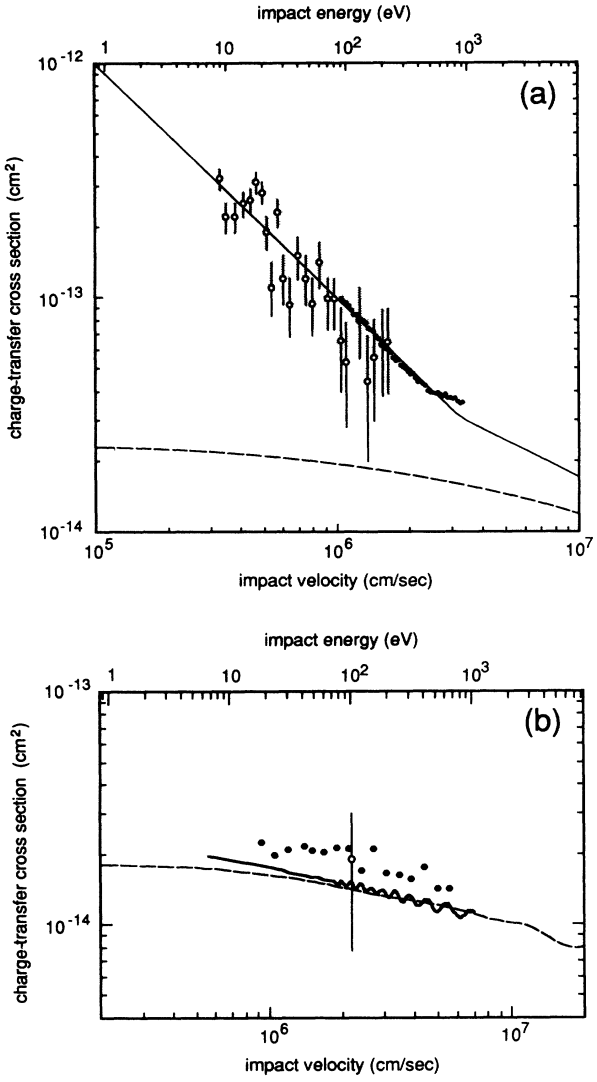

FIG. 3. (a) Dependence of charge-transfer cross section in Gd-Gd$^+$ collisions on impact velocity (energy). Solid circles and open circles in the shaded area were obtained by measurement of the charge-transferred ions and of the attenuated primary-ion beam, respectively. For solid circles, the fluctuation of data in each laser shot is smaller than the size of the symbols in the figure. A dashed line denotes the calculational result for resonant charge transfer (Ref. [1]); a solid line is the result of a simple superposition of the resonant and capture-type probabilities resulting in charge transfer. (b) Dependence of the charge-transfer cross section in Ca-Ca$^+$ collisions on impact velocity (energy). Solid circles and an open circle with an error bar were obtained by measurements of the charge-transferred ions and of the attenuated primary-ion beam, respectively. A dashed line denotes the calculational result for resonant charge transfer (Ref. [1]). The thick solid line shows the experimental result obtained by Panev *et al.* (Ref. [5]).

$4f^7 5d 6s^2\,{}^9D_2$ (ground state), ${}^9D_3$ (215 cm^{-1}), ${}^9D_4$ (533 cm^{-1}), ${}^9D_5$ (999 cm^{-1}), and ${}^9D_6$ (1719 cm^{-1}) [6] in the ratios of 20%, 23%, 23%, 20%, and 13%, respectively. The internal energy of the atom is, therefore, in the range 0–0.21 eV. The photon energy of the ArF laser is 6.42 eV, which is 0.27 eV higher than the ionization potential of the Gd-atom ground state. Consequently, the internal energy of the ions produced in the atomic beam by laser photoionization (autoionization) is considered to be, at most 0.48 eV in the present experiment. In the range 0–0.48 eV, there are the Gd II states of $4f^7 5d 6s\,{}^{10}D_{5/2,7/2,9/2,11/2,13/2}$, ${}^8D_{3/2,5/2,7/2}$, and $4f^7 6s^2\,{}^8S_{7/2}$ [6]. However, these characteristics do not influence the resonant-charge-transfer cross section more than the accuracy of the present result [7].

V. UNCERTAINTIES IN THE RESULTS

The cross sections were determined by the values of N/N_0, n, and l. Note that the absolute value of N_{CT} is not necessary here, as was mentioned above. The accuracy of the measurements of these values cause the uncertainties in the obtained cross sections. The uncertainties of the cross section measured by the attenuation method is given by

$$\left|\frac{\Delta\sigma}{\sigma}\right| \le \left|\frac{\Delta n}{n}\right| + \left|\frac{\Delta l}{l}\right| + \left[\left|\frac{\Delta N}{N}\right| + \left|\frac{\Delta N_0}{N_0}\right|\right]\left|\ln\left[\frac{N}{N_0}\right]\right|^{-1}.$$

In the present apparatus the ion beam is produced by laser photoionization in an atomic beam. The laser power is so high that its fluctuation does not affect the ion-beam density, and the ion-beam density fluctuates as much as the atomic-beam density. Though both the injected primary ion beam and the attenuated ion beam can be accurately measured, they cannot be measured simultaneously. During each measurement the atomic-beam density is probably changed. Therefore the uncertainties of the ion beams, $|\Delta N/N|$ and $|\Delta N_0/N_0|$, should be equal to that of the atomic-beam density, $|\Delta n/n|$. Then,

$$\left|\frac{\Delta\sigma}{\sigma}\right| \le \left[1+2\left|\ln\left[\frac{N}{N_0}\right]\right|^{-1}\right]\left|\frac{\Delta n}{n}\right| + \left|\frac{\Delta l}{l}\right|.$$

In the present experiment, the atomic-beam density was measured with the vapor monitor, which has a time resolution of only 2 sec. In a separate experiment, the atomic-density fluctuation was investigated by measuring the fluorescence from the atomic beam, which was induced with a cw dye laser. The energy intensity of the fluorescence fluctuated in the range of ±1%. This means that $|\Delta n/n| = 0.01$, because the cw-laser power fluctuation is much less than it is. Concerning the interaction length, that is, the atomic-beam width, it is not sensitive to the atomic-beam density, and its fluctuation is negligible, while the measurement accuracy is ±1%. Then, $|\Delta l/l| = 0.01$. As a result, the uncertainties in the cross sections are dominantly determined by the first term in the above equation. For example, $|\Delta\sigma/\sigma| = 0.10$ for $\sigma = 3\times10^{-13}$ cm^2 and 0.80 for 3×10^{-14} cm^2. These are shown by error bars in Fig. 3, and correspond to the full width at half maximum of the static distribution of measured values (2000 data points at each velocity). On the other hand, the relative uncertainty of the cross section obtained using the method of charge-transferred-ion measurement is given by

$$\left|\frac{\Delta\sigma}{\sigma}\right| \le \left|\frac{\Delta n}{n}\right| + \left|\frac{\Delta l}{l}\right| + \left|\frac{\Delta(N_{CT}/N)}{N_{CT}/N}\right| = 2\left|\frac{\Delta n}{n}\right| + \left|\frac{\Delta l}{l}\right|,$$

and this value is estimated to be 0.03.

VI. DISCUSSION

The present results were compared with cross sections of other elements investigated experimentally in many studies since the 1930s [1], and with the cross-section–impact-velocity curve obtained by calculating resonant processes. The cross section for resonant charge transfer at low velocities in the collision of an ion X^+ with the corresponding neutral atom X are determined mainly by the potential curves of the low-lying states of the molecule $X_2{}^+$, which is formed temporarily during the collision. These potential curves are significantly related to the ionization potential of the neutral atom X. Figure 4 shows the cross sections of elements investigated in the past as a function of their ionization potentials, at impact velocities of 1×10^6 and 3.5×10^6 cm/sec [1]. From the correlation, the cross section σ can be related to the ionization potential I by $\sigma = \sigma_0(I/I_0)^{-1.5}$, where $\sigma_0 = (3.9-7.5)\times10^{-15}$ and $(2.1-5.1)\times10^{-15}$ cm^2 at 1×10^6 and 3.5×10^6 cm/sec, respectively, and $I_0 = 13.559$ eV. The present cross section for Gd is about 5 times larger than that predicted by this relation at 1×10^6 cm/sec, while the cross section is relatively close to it at 3.5×10^6 cm/sec. On the other hand, the cross section of Ca at each velocity is nearly equal to that given by this relation. The cross-section–velocity curve for resonant charge transfer was calculated using the impact-parameter and close-coupling methods using the Hartree-Fock-Slater wave function [1]. The reasonableness of this calculation can be seen in Fig. 4, in which the calculational results for all nontransition elements are included and are in fairly good agreement with experimental data. The result is given by a dashed line in Fig. 3. The present experimental result for Gd shows not only a larger cross section than the prediction, but also a different impact-velocity dependence, while that for Ca shows good agreement with prediction. Especially for Gd in the low-velocity range, the cross section is inversely proportional to the impact velocity.

For Gd, when the charge-transfer cross section is assumed to result from both a resonant process and some capture-type process, of which the cross section is inversely proportional to the velocity, the cross section is given by [8]

$$\sigma=\pi b_2^2+(\pi/2)(b_1^2-b_2^2)S(b_1-b_2)\ ,$$

$$S(x)=\begin{cases}1 & (x>0)\\ 0 & (x<0)\ ,\end{cases}$$

where b_1 and b_2 are impact parameters at which the probabilities of charge transfer become zero; these parameters are related to the cross sections of resonant and capture processes by

$$\sigma_r=(\pi/2)b_1^2,\quad \sigma_c=\pi b_2^2=A/v\ ,$$

respectively, where A is a constant. When A is determined so that σ agrees with the experimental result at low velocity, the σ-v curve fits the present result well in all of the present velocity ranges [solid line in Fig. 3(a)]. It is well known that Langevin capture [9] becomes dominant in the electron-transfer process, in the low-energy region, i.e., thermal to a few electron volts, and the cross section σ_L is related to the relative kinetic velocity v,

$$\sigma_L=\pi(2e^2\alpha)^{1/2}/v\ ,$$

where e is the electron charge and α is the polarizability of the neutral. If $\sigma_c=\sigma_L$, for Gd, $\alpha=2.9\times10^5$ Å^3. This value is about 4–5 orders magnitude larger than those of atoms studied in the past [10].

The cross section for uranium measured by Niki *et al.* [11] is also several times larger than that predicted by the resonant-charge-transfer process. Mizushima explains this large cross section as follows [12]. The ground state of the U atom is the $5f^3\ (^4I)6d7s^2\ ^5L_6$ state, where the core electrons, including $5f^3$, are coupled to be in the ^4I state [13]. Only 0.08 eV above the ground state is the lowest excited state, which is the $5f^3(^2H)6d7s^2\ ^5K_5$ state [13]. Although the matrix element of the collision energy between these two core states may be small, the very small energy difference must make the transition between these two core states very easy. Thus, the U gas can be regarded as a mixture of two kinds of U atoms (and ions) with ^4I and ^2H cores. In the U ion the ground state is $5f^3(^4I)7s^2\ ^4I_4$, though the lowest excited state is $5f^3(^4I)6d7s\ ^6L_5$, with an excitation energy of only 0.04 eV [14]. Thus, the ionization produced by removing a $7s$ electron is as important as that produced by removing a $6d$ electron. Distinguishing these two kinds of U atoms or ions, and considering that one of the $7s$ electrons contributes to charge transfer in the same way as the $6d$ electron, eight processes between U and U^+ are actually observed, and the cross section must be about eight times that of the individual process, as the cross sections of eight processes are nearly equal to each other.

This successful theoretical model, however, cannot be applied to the explanation of the present result for Gd. The ground state of the Gd atom is $4f^7(^8S)5d6s\ ^9D_2$ state, and in the excited states, the state of the core consisting of seven $4f$ electrons is only ^8S. The Gd atom has only one kind of core state. In the Gd ion the ground state is $4f^7(^8S)5d6s\ ^{10}D_{5/2}$, and the excited state of $4f^7(^8S)6s^2\ ^8S_{7/2}$ can be seen 0.427 eV above the ground state, which is much higher than that of the U ion. Therefore the enlargement of the cross section seen in the U case is impossible in the Gd case.

If the assumption using Langevin capture is applied to the U result, it gives $\alpha=3.5\times10^5$ Å^3. It cannot yet be concluded that the polarizabilities for gadolinium and uranium are so large that they are sensitive to collision in the present velocity range. However, more detailed studies of the polarizabilities of transition elements and their

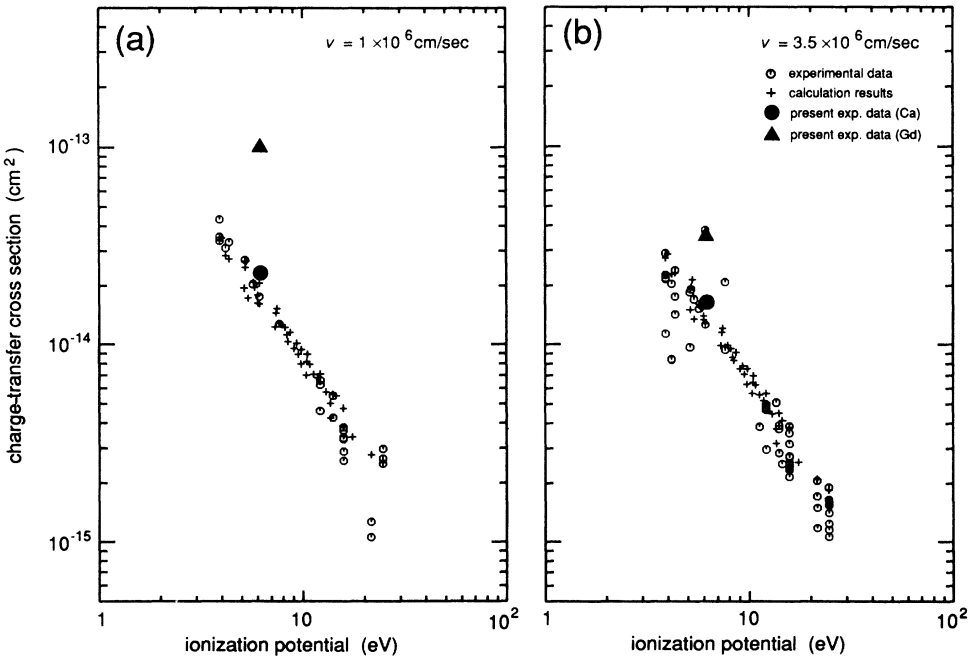

FIG. 4. Cross sections investigated in the past as a function of the ionization potentials of elements at impact velocities of (a) 1×10^6 and (b) 3.5×10^6 cm/sec (Ref. [1]). Open circles and +'s are from the compiled experimental data and calculational results in Ref. [1], respectively; triangles and solid circles are the present results for Gd and Ca, respectively.

sensitivity to collision processes necessarily should be continued.

VII. SUMMARY

The cross section of symmetric charge transfer between atoms and positive atomic ions for Gd as a function of impact energy in the range 10–1000 eV was obtained by a crossed-beam technique, which featured a pulsed ion beam produced by laser photoionization in atomic gas beam. Coupling the technique of charge-transferred-ion measurement with the primary-ion-attenuation method, the cross sections were successfully measured without any assumption or any atomic data. The test measurement of Ca lent confidence to the present measurement technique. While the obtained cross sections of Gd in the range 1.5×10^6–3.5×10^6 cm/sec are close to that predicted by the resonant process, the cross sections in the range 3.5×10^5–1.5×10^6 cm/sec are inversely proportional to the impact velocities. The cross-section-velocity curve fitted well with that obtained from the superposition of the resonant and capture-type probabilities resulting in charge transfer.

ACKNOWLEDGMENTS

The authors are grateful to Dr. H. Niki and Professor N. Nakashima for discussion and comments. We wish to thank Professor Y. Kato and Professor M. Mizushima for their interest in and encouragement for our work. We thank C. Frantz for reading the manuscript. This work was supported, in part, by the Matsuo Foundation.

[1] S. Sakabe and Y. Izawa, At. Data Nucl. Data Tables **49**, 257 (1991). In this article, all the experimental data on symmetric charge-transfer cross sections studied since the 1930s are compiled, and the calculational results of resonant-charge-transfer cross sections for all nontransition elements are tabulated.

[2] P. T. Greenland, Contemp. Phys. **31**, 405 (1990); S. Sakabe, Y. Izawa, T. Yamanaka, K. Nishihara, S. Nakai, and C. Yamanaka, Institute of Laser Engineering, Osaka University, Quarterly Progress Report No. 33, 1991 (unpublished).

[3] S. Sakabe, Y. Izawa, M. Hashida, T. Naka, T. Sudo, T. Mochizuki, T. Yamanaka, S. Nakai, and C. Yamanaka, Rev. Sci. Instrum. **61**, 3678 (1990).

[4] R. C. Stern and N. C. Lang, J. Chem. Phys. **70**, 1802 (1979).

[5] G. S. Panev, A. N. Zavilopulo, I. P. Zapesochnyi, and O. B. Shpenik, Zh. Eksp. Teor. Fiz. **67**, 47 (1974) [Sov. Phys.—JETP **40**, 23 (1975)].

[6] W. C. Martin, R. Zalubas, and L. Hagan, *Atomic Energy Levels*, Natl. Bur. Stand (U.S.) Spec. Publ. No. NSRDS-60 (U.S. GPO, Washington, DC, 1978).

[7] M. Kimura and T. Watanabe, J. Phys. Soc. Jpn. **31**, 1600 (1971).

[8] F. A. Wolf and B. R. Turner, J. Chem. Phys. **48**, 4226 (1968).

[9] P. Langevin, Ann. Chem. Phys. **5**, 245 (1905).

[10] G. S. Chandler and R. Glass, J. Phys. B **20**, 1 (1987).

[11] H. Niki, Y. Izawa, H. Ohtani, and C. Yamanaka, Trans. Inst. Elect. Eng. Jpn. **102**, 45 (1982).

[12] M. Mizushima, Jpn. J. Appl. Phys. **27**, 449 (1988).

[13] J. Blaise and L. J. Radziemski, Jr., J. Opt. Soc. Am. **66**, 644 (1976).

[14] L. R. Kahn, P. J. Hay, and R. D. Cowan, J. Chem. Phys. **68**, 2386 (1978).

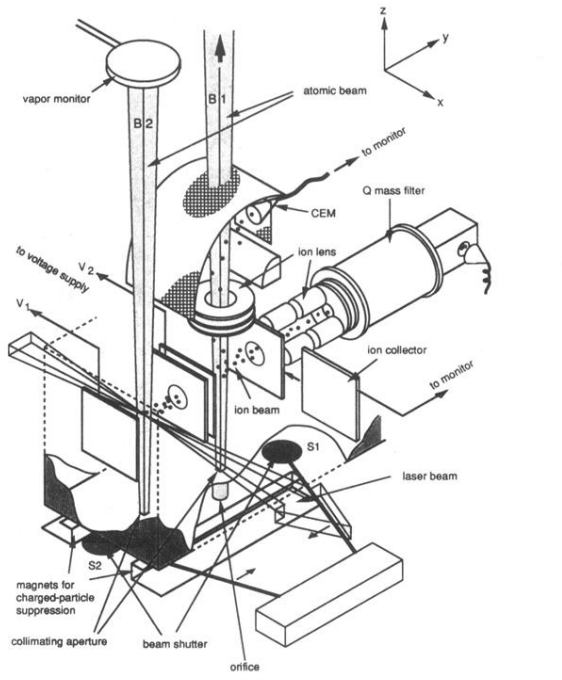

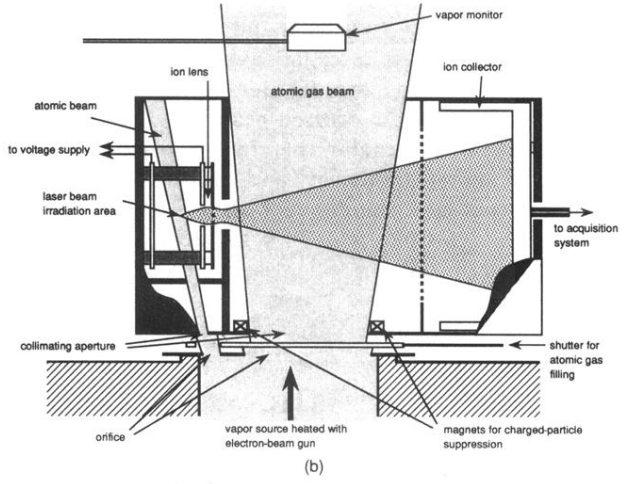

FIG. 1. Schematic views of the apparatus for measuring of charge-transfer cross sections using a crossed-beam technique. The two atomic beams emerged from orifices on the floor separating the first and second chambers. The crucible and electron-beam gun for atomic vapor production are located in the first chamber (not seen in this figure), which is situated below the second chamber. A laser beam is injected into one of the atomic beams, which photoionizes it, and the ions produced are extracted and focused onto another atomic beam. Both (a) the charge-transferred ions and (b) the attenuation of the primary ions are measured. In (a) the charge-transferred ions are guided by curved electrodes through an ion lens, and are detected by a ceramic-type electron multiplier. In (b), the injected primary ions and the attenuated ions are alternately detected by a Faraday cup, closing and opening a shutter for the atomic-beam gas, respectively.

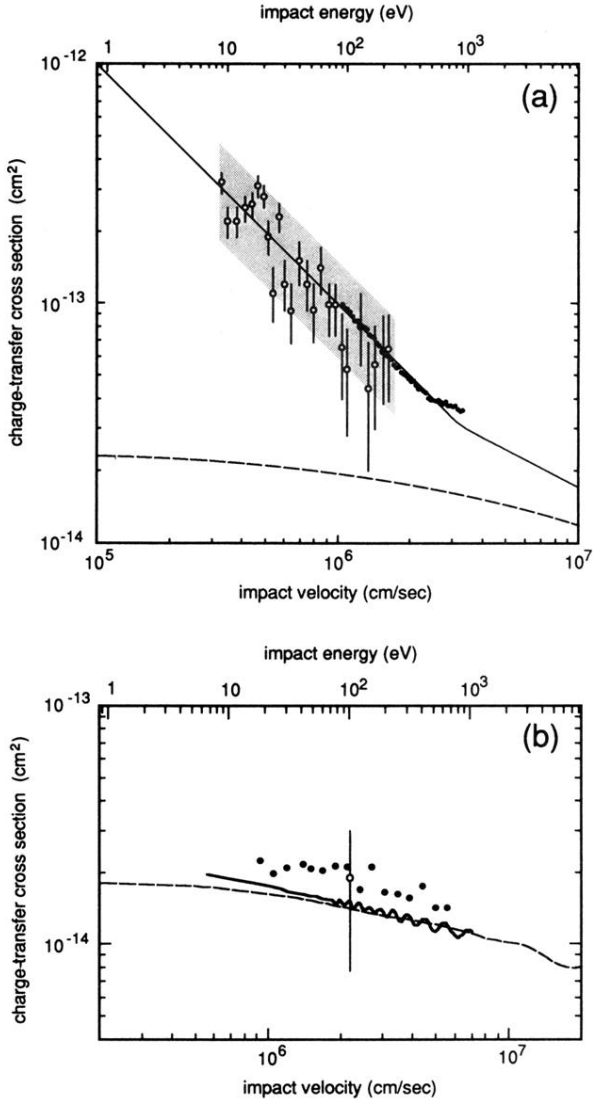

FIG. 3. (a) Dependence of charge-transfer cross section in Gd-Gd^+ collisions on impact velocity (energy). Solid circles and open circles in the shaded area were obtained by measurement of the charge-transferred ions and of the attenuated primary-ion beam, respectively. For solid circles, the fluctuation of data in each laser shot is smaller than the size of the symbols in the figure. A dashed line denotes the calculational result for resonant charge transfer (Ref. [1]); a solid line is the result of a simple superposition of the resonant and capture-type probabilities resulting in charge transfer. (b) Dependence of the charge-transfer cross section in Ca-Ca^+ collisions on impact velocity (energy). Solid circles and an open circle with an error bar were obtained by measurements of the charge-transferred ions and of the attenuated primary-ion beam, respectively. A dashed line denotes the calculational result for resonant charge transfer (Ref. [1]). The thick solid line shows the experimental result obtained by Panev *et al.* (Ref. [5]).